Patient-specific finite element simulation of the insertion of guidewires during an EVAR procedure: towards clinically relevant indicators

J. Gindre, A. Bel-Brunon, Alain Combescure, Pascal Haigron, M Rochette, Antoine Lucas

4th International Conference on Computational and Mathematical Biomedical Engineering – CMBE2015
29 June - 1 July 2015, France
P. Nithiarasu and E.Budyn (Eds.)

PATIENT-SPECIFIC FINITE ELEMENT SIMULATION OF THE INSERTION OF GUIDEWIRES DURING AN EVAR PROCEDURE: TOWARDS CLINICALLY RELEVANT INDICATORS

J.Gindre[1,2,3,5], A.Bel-Brunon[1], A.Combescure[1], P.Haigron[2,3], M.Rochette[5], A.Lucas[2,3,4]
[1] LaMCoS, UMR CNRS 5259/ INSA-LYON, Villeurbanne 69621, France, juliette.gindre@ansys.com
[2] LTSI, Université Rennes 1, Rennes 35000, France
[3] INSERM U1099, Rennes 35000, France
[4] CHU Rennes, Vascular Surgery Unit, Rennes 35000, France
[5] ANSYS France, Montigny-le-Bretonneux 78180, France

SUMMARY

This work presents an explicit FE method to compute the deformation of an aorto-iliac structure induced by endovascular extra-stiff guidewires. The mechanical model takes into account the nonlinear behavior of the arterial wall, the prestressing effect induced by blood pressure and the mechanical support of the surrounding organs and structures. The simulation results are evaluated against 3D imaging data acquired during the surgical procedure on 17 patients. Then the results can be used to derive clinically relevant quantities, like arterial segment shrinkage, length of the stent-graft to be deployed, displacement of important anatomical points.

Key words: *simulation, biomechanics, EVAR*

1 INTRODUCTION

EndoVascular Aneurysm Repair (EVAR) is a commonly-used mini-invasive technique which has gained increasing popularity over the last 10 years. It relies on the exclusion of the aneurysm sac by means of the femoral introduction of one or more stent grafts and their deployment inside the aneurysm. During the intervention, insertion of extra-stiff guidewires often leads to the straightening of vascular structure. During this process, the vascular structure undergoes major deformations [1], which can have major consequences. Straightening tortuous arteries may lead to shrinkage of the arterial segments compared to the preoperative anatomy, thus calling into question the initial sizing of the stent grafts. It can also induce major movements of anatomical markers such as the ostia of the digestive arteries, leading, in the most critical cases, to a risk of covering a secondary artery [2]. Conversely, in some cases, the tools are incapable of straightening excessively calcified and tortuous arteries, thus precluding the delivery of the stent graft, which usually leads to an amendment of the procedure or to its cancellation [3].

Arterial deformations caused by the endovascular equipment during surgery depend on multiple factors, such as the morphology of the arteries, the state and degree of calcification of the arterial wall, and also the types of devices used. Today, their prediction relies mainly on the surgeon's experience. Numerical simulation appears to be an appropriate tool to anticipate the complications mentioned above[4][5]. Its use in the preoperative phase could give the practitioner more objective and more useful indicators when planning the procedure in order to reduce the risks of intraoperative and postoperative complications.

Here, we present the development of a method for the simulation of the deformation of the vascular structure due to the insertion of extra-stiff guidewires during an EVAR procedure using an explicit finite-element software. The simulation results are evaluated against 3D imaging data acquired during the surgical procedure on 17 patients. Once the predictive capability of the simulation is attested, we can derive clinically relevant quantities, like arterial segment shrinkage, length of the

stent-graft to be deployed, guidewire curvature, and displacement of important anatomical points like ostia of secondary arteries.

2 METHODOLOGY

2.1 Biomechanical model

The vascular geometry modeled in the simulations corresponds to an aorto-iliac structure including the abdominal aorta and the common and external iliac arteries as far as the femoral bifurcations. The models are meshed with triangular shell elements. The behavior of the arterial wall is modeled using the polynomial, nonlinear and isotropic hyperelastic potential defined by Equation (1):

$$W = C_{10}(I_1 - 3) + C_{20}(I_1 - 3)^2 \quad (1)$$

with $C_{10} = 0.005\ MPa$ and $C_{20} = 0.2\ MPa$. Elements corresponding to calcification plaques are assigned linear elastic properties (Young's modulus $E = 40\ MPa$, Poisson's ratio $\upsilon = 0.4$). Intraluminal thrombus was not represented in the models.

The effect of surrounding organs and structures is modeled by a visco-elastic support on the entire surface of the vascular mesh. The resulting nodal load is defined by equation (2):

$$\vec{\boldsymbol{f}}_{\boldsymbol{ext}} = \vec{\boldsymbol{t}}_{\boldsymbol{ext}}.dS = (-k\vec{\boldsymbol{u}} - c\vec{\boldsymbol{v}} + p\vec{\boldsymbol{n}}).dS \quad (2)$$

where $\vec{\boldsymbol{u}}$ is the displacement of the considered mesh node, $\vec{\boldsymbol{v}}$ the velocity of the node, $\vec{\boldsymbol{n}}$ the vector normal to the surface at this node, k the surfacic stiffness coefficient of the support, c the surfacic viscosity coefficient of the support, p the external pressure, $\vec{\boldsymbol{f}}_{\boldsymbol{ext}}$ the resultant external force vector and dS the elementary surface. The elastic stiffness k which represents the support from the surrounding organs and tissues is a function of the vascular segments considered: healthy aorta (k_1), aneurysmal aorta (k_3), common iliac arteries (k_5) and external iliac arteries (k_7). An elastic stiffness k_{iliac} is also added locally at the beginning of the internal iliac arteries in order to represent the limited mobility of these points. The relatively stationary proximal and distal extremities are modeled by a zero-displacement condition over the three outer borders of the mesh.

The prestressing effect of blood pressure is also taken into account. We use an iterative method similar to the one described by Bols and al. [6] to determine a new geometry which corresponds to a stress-free state often called "zero-pressure geometry". Then, at the start of the simulation, this geometry is subjected to the internal pressure, which enables one to recover the reference geometry as observed on the CT-scan images, except that it now incorporates the prestress due to blood pressure. Then we process with the simulation of guidewire insertion

The guidewires represented in the simulation are Lunderquist "extra-stiff" (Cook), they are modeled using 189 4mm-long two-noded beam elements with linear elastic properties (Young's modulus E =180 GPa , Poisson's ratio υ = 0.3) The tools are pushed at the distal end of the external iliac arteries by prescribing a velocity at their lower end until they are fully inserted in the vascular structure.

2.2 Results validation and derivation of clinically relevant data

As no literature data are available concerning the support parameters $\mathrm{k}_1, \mathrm{k}_3, \mathrm{k}_5, \mathrm{k}_7$, their values were first calibrated through sensitivity analysis on one patient-specific case (*P0*), the results are then blindly evaluated on 17 other patient-cases to assess the method robustness and predictive capability. For each patient, either a 3D rotational acquisition or multi-incidence 2D acquisitions are done under fluoroscopy imaging which allows reconstructing the 3D position of the real intraoperative guidewire. After registration of the intraoperative data into the simulation coordinate system, the positions of the simulated guidewire and the real guidewire can be compared. The metric used to measure the error between the simulated and the real guidewire is the Modified Hausdorff Distance (MHD)[7]. The simulation error is deemed acceptable for targeted clinical applications when less than 3mm.

Then several clinically relevant quantities are derived from the simulation results. The change in common iliac length is measured as the length difference between the preoperative centerline and

the centerline of the artery deformed by the guidewire. The deployment length is defined by the length of the guidewire portion comprised between the renal arteries ostia and the internal iliac artery ostium and corresponds to the length on which the stent-grafts are going to be deployed. A measure of the guidewire curvature once inserted into the vascular structure is estimated by the computation of its flexural energy normalized by its length. Finally, the displacement of left and right renal arteries' ostia is measured between the preoperative and the deformed configurations.

3 RESULTS AND CONCLUSIONS

Fig. 1 illustrates on 4 patients the comparison between the real and simulated final guidewire position. Tab.1 displays the average MHD of 17 patients after calibration of the model on patient *P0*. It shows that, while the model parameters have been optimized to minimize the MHD of a single patient (*P0*), the simulation results are acceptable for clinical application (MHD < 3mm) for 6 cases and still reasonable (MHD < 5mm) for 6 other cases. The predictive capability of the model is therefore rather good in spite of a rather small number of patient-specific parameters (mostly the geometry so far).

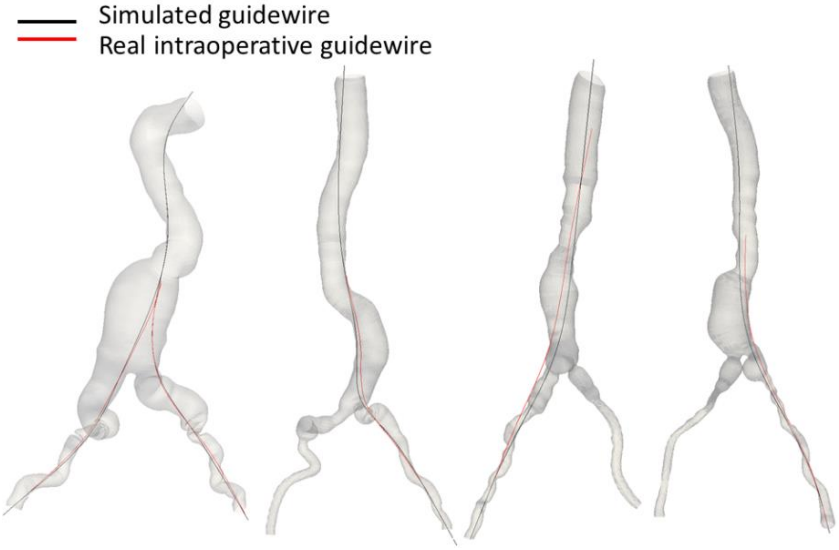

Figure 1*:* Illustration of real and simulated guidewires position comparison on 4 patients

Patient id	MHD (mm)	Patient id	MHD (mm)
1	4,13	10	4,69
2	5,68	11	2,31
3	7,93	12	3,24
4	1,61	13	3,78
5	2,79	14	2,27
6	9,83	15	2,47
7	5,14	16	4,95
8	6,85	17	3,85
9	2,98	**mean**	**4,38**

Table 1: Modified Hausdorff Distance between real and simulated guidewire for the 17 patients

Tab. 2 displays the computed values for clinically relevant data: it shows that numerical simulation can predict some rather large variations in the vascular geometry due to tools insertion. Along with the final deformed configuration of the vascular structure that can be used to improve intraoperative visualization and guidance, the preoperative computation of those quantities could help surgeons in planning their interventions by providing more objective arguments for sizing and choice of the stent-grafts and by anticipating possible intraoperative complications. To improve the predictive capability of the model, future work will focus on calibrating the model parameters

using a larger number of cases. A sensitivity analysis based on a large number of cases will therefore help determining which parameters require a patient-specific determination.

Patient id	Common iliac Length change (mm)	Deployment length (mm)	Guidewire curvature (flexural energy by unit length in J/mm)	Ostia displacement (mm) Left / Right	
1	-21,6	173	9,1	1,2	0,5
2	-1,6	155	2,4	0,9	0,3
3	-4	154	1,9	0,9	0,7
4	-11,8	170	5,9	1,6	1,3
5	-1,4	142	4,3	0,8	0,6
6	-8,7	146	11,7	1,05	0,45
7	-8,2	144	5,5	1,7	1,2
8	-6,7	159	2,6	0,7	0,2
9	-8,6	181	6,1	0,6	0,6
10	-7,8	157	5	1,5	0,7
11	-6,6	184	2,3	0,4	0,6
12	-2,6	144	3,3	0,6	1
13	-9,7	148	12,3	2,6	1,7
14	-7,5	169	4	0,3	0,9
15	-4,7	137	5,9	1,2	1,7
16	-0,4	203	6,4	1,1	1,3
17	-10,3	177	7,5	0,6	0,8
mean	**-7,19**	**161,35**	**5,66**	**1,04**	**0,86**

Table 2: Clinically relevant quantities derived from simulation results for the 17 patients

REFERENCES

[1] D. L. Dawson, J. C. Hellinger, T. T. Terramani, S. Najibi, L. G. Martin, and A. B. Lumsden. Iliac Artery Kinking with Endovascular Therapies: Technical Considerations. *Journal of Vascular and Interventional Radiology*, 13(7):729‑733, 2002.

[2] B. Maurel, A. Hertault, T. M. Gonzalez, J. Sobocinski, M. Le Roux, J. Delaplace, R. Azzaoui, M. Midulla, and S. Haulon. Evaluation of Visceral Artery Displacement by Endograft Delivery System Insertion. *Journal of Endovascular Therapy*, 21(2):339‑347, 2014.

[3] V. J. Gokani, N. G. Fishwick, E. Choke, M. J. Bown, and R. D. Sayers. 'Trial of Stiff Guidewire': A Useful Adjunct to Determining Suitability for Endovascular Aneurysm Repair. *European Journal of Vascular and Endovascular Surgery*, 44(5):527, 2012.

[4] A. Kaladji, A. Dumenil, M. Castro, A. Cardon, J.-P. Becquemin, B. Bou-Saïd, A. Lucas, and P. Haigron. Prediction of deformations during endovascular aortic aneurysm repair using finite element simulation. *Computerized Medical Imaging and Graphics*, 37(2):142‑149, 2013.

[5] A. Dumenil, A. Kaladji, M. Castro, S. Esneault, A. Lucas, M. Rochette, C. Goksu, and P. Haigron.Finite-Element-Based Matching of Pre- and Intraoperative Data for Image-Guided Endovascular Aneurysm Repair. *Biomedical Engineering, IEEE Transactions*, 60(5):1353‑1362, 2013.

[6] J. Bols, J. Degroote, B. Trachet, B. Verhegghe, P. Segers, and J. Vierendeels. A computational method to assess the in vivo stresses and unloaded configuration of patient-specific blood vessels. *Journal of computational and Applied mathematics*, 246:10‑17, 2013.

[7] M.-P. Dubuisson and A. K. Jain. A modified Hausdorff distance for object matching, *Pattern Recognition*, 1:566‑568, 1994.